

## A Method to correct HILLAS parameters of Imaging Cherenkov telescope data taken at different background light levels

M. Kestel, D. Kranich, and E. Lorenz

MPI für Physik, München, Germany

**Abstract.** During observations of  $\gamma$  showers with Cherenkov telescopes the background light conditions can vary, resulting in shifts of the values of the HILLAS image parameters.

These changes increase when working with low 'tail' cuts for image cleaning.

Here we present a first approach for correcting some of the variations. First tests of the method are carried out with HEGRA CT1 data.

### 1 Introduction

Imaging Cherenkov telescopes are currently the most successful instruments for ground based  $\gamma$ -astronomy. The main breakthrough was achieved by the imaging technique based on the HILLAS image parameters (Hillas, 1985), allowing for an efficient  $\gamma$ -hadron separation. Cuts for  $\gamma$ -hadron separation were determined from Monte Carlo simulated showers, respectively from real data which include a prominent source, such as the Crab.

The combination of the atmosphere and a Cherenkov telescope is basically a fully active calorimeter without enclosure. The open structure is sensitive to a variety of external light background sources and changes of optical transmission of the atmosphere.

In order to prepare raw shower images for the analysis it is necessary to apply so-called 'tail cuts' to reject pixels with low physical signal content. Low tail cuts normally increase image differences between  $\gamma$  and hadron showers, while high tail cuts are resulting in more stable image parameters but also in reduced separation power.

In the standard CT1 analysis (see e.g. Petry (1997)) the RMS variation of the ADC pedestal values is taken as a measure of the night sky background (NSB) light level. The cuts are normally 2.5 times the RMS of the noise. The procedure is called 'dynamic image tailcut cleaning'.

The image parameters *WIDTH* and *LENGTH* are the most sensitive ones to changes of the tail cut.

As background conditions are constantly varying during observations and thus influence the image parameters, one could in principle consider these changes in the Monte Carlo simulation and determine a large number of cuts for all variants of background.

The other alternative is to correct the observed images, respectively the image parameters, such that the corrected parameters resemble those for a reference set of background conditions, i.e., one can work with one set of cuts.

The basic idea to extract these corrections is to use the changes of the hadronic background images and to renormalise them to the reference background, i.e. multiply the *WIDTH* and *LENGTH* by a correction factor. In only a few minutes of observation time plenty of hadronic events are collected which allow to determine these corrections with high precision.

In principle also the threshold and therefore the flux can change significantly due to changes in the tail cuts, but this is not yet considered.

Normalising image parameter distributions should make the  $\gamma$ -hadron separation more stable. Here we describe a first attempt to correct data and making them more robust. The ideas were tested on data recorded with the HEGRA CT1 telescope. For the description of CT1 see e.g. Mirzoyan et al. (1994); Cortina et al. (1999).

Sources of the observed variations are:

- (i) Observation of sources in sky regions of lower / higher background level due to more or fewer stars in the field of view (FOV). Difficulties are expected when cuts that have been optimised on a source in the 'brighter' galactic plane are applied to a source outside the galactic plane.
- (ii) Increased night sky background due to zodiacal light, faint light during dusk or dawn, faint moon light or remote lightning.

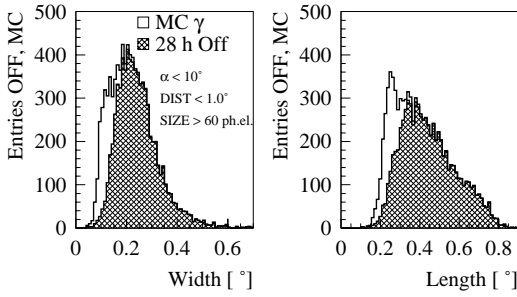


**Fig. 1.** *WIDTH* and *LENGTH* distributions of Monte Carlo (MC)  $\gamma$ -showers on top of Offdata. The Monte Carlo data correspond to a  $\gamma$  signal collected over 28 hours on a 20-Crab-flux level and with a power law index of  $-2.7$ . Selecting  $\alpha < 10^\circ$ ,  $DIST < 1.0^\circ$  and the  $SIZE > 60$  photo electrons already strongly focuses on  $\gamma$ -like events.

- (iii) Variable man-made background light.
- (iv) Small losses due to variable dust or haze content in the atmosphere. These effects do not necessarily show up as a reduced trigger rate.
- (v) Variable electromagnetic noise pickup from nearby power supplies or motors.
- (vi) Mirrors, PM windows affected by temporary deposition of dew or dust.
- (vii) Varying ground albedo due to snow or plant growth.

This paper is organised as follows:

The influence of night sky background light on the determination of the image parameters *WIDTH* and *LENGTH* is shown for Monte Carlo  $\gamma$ -ray showers in the first part of Section 2. In the second and the third part recent raw datasets from Crab and Mkn 421 observations, respectively, are examined. Section 3 presents an attempt for a correction, Section 4 discusses the improvements and further ideas.

## 2 Effects of variable Background on Image Parameters

The influence of variable background conditions on image parameters is strongest for *WIDTH* and *LENGTH*, which are also the most important image parameters for the  $\gamma$ -hadron separation.

*WIDTH* and *LENGTH* are defined as the RMS of the 'images' along the main axis of the shower image (*LENGTH*) and orthogonal to the main axis (*WIDTH*). Smaller RMS values are calculated when more of the outer pixels are excluded from the image parameter calculation due to a higher tailcut.

Figure 1 illustrates the well known situation of  $\gamma$ -hadron distributions: Monte Carlo (MC)  $\gamma$ -events (unshaded areas) have a smaller *WIDTH* (left plot) and *LENGTH* (right plot) than hadrons, here shown from 28 hours of Off-data.

Any fixed cut will result in a large variation if the *WIDTH* (*LENGTH*) jitters with the NSB.

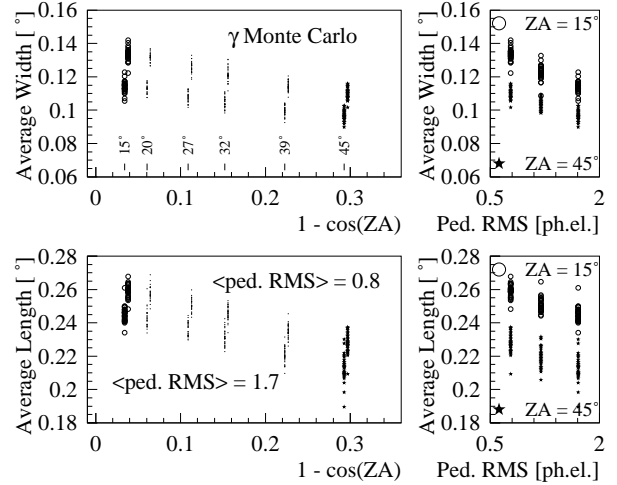


**Fig. 2.** Average *WIDTH* (top) and *LENGTH* (bottom) as a function of the zenith angle (ZA) of the simulation (left hand side) for two different levels of NSB in the simulation. The upper points correspond to a pedestal RMS of 0.8 photo electrons, the lower points to 1.7 photo electrons. In the plots on the right hand side the averaged quantities are drawn for the two extreme ZAs as a function of the three simulated pedestal RMS values. See text.

### 2.1 Simulation of NSB Effects on Monte Carlo $\gamma$ -Images

To further illustrate the problem we have simulated  $\gamma$ -events with different levels of NSB; here we use the word NSB for all variable background listed above as items (i) through (vii).

The average values of *WIDTH* and *LENGTH*, as shown in Figures 2 through 4 have been defined as the average value over all events in a run that fulfill the following criteria:

- (i)  $SIZE \geq 60$  ph.el.,
- (ii)  $DIST \leq 1.0^\circ$ , and
- (iii)  $ALPHA \leq 60^\circ$ .

(The conditions (ii) and (iii) are introduced to avoid camera edge effects.)

One data point in Figure 2 represents on average  $\sim 200$  Monte Carlo events.

For the simulations the mean pedestal RMS has been calculated from real data with different night sky background.

Figure 2 shows the average *WIDTH* (top panel) and the average *LENGTH* (bottom panel) as a function of the simulated zenith angle on the left hand side for two different levels of NSB, i.e. 0.8 ph.el. (upper points) and 1.7 ph.el. pedestal RMS (lower points), drawn slightly shifted against each other.

The right plots show the average *WIDTH* and *LENGTH* as a function of the pedestal RMS values for the two zenith angles  $15^\circ$  (open circles, upper points) and  $45^\circ$  (stars, lower points).

It can be seen that the Monte Carlo *WIDTH* and *LENGTH* scale inversely to both the zenith angle and the level of the simulated night sky background.

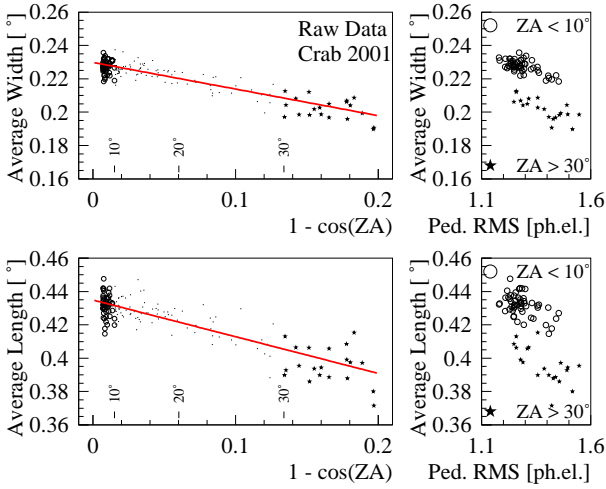


**Fig. 3.** Average *WIDTH* (top) and *LENGTH* (bottom) of raw data from CT1 Crab observations in 2001 as a function of the zenith angle (ZA) of the observation on the left hand side and as a function of the pedestal RMS of the respective run on the right hand side. The averaging has been made before any  $\gamma$ -hadron separation cuts. One point is drawn per datarun of  $\sim 20$  minutes duration.

The zenith angle affects the average *WIDTH* and *LENGTH* purely through geometry effects while the NSB level acts through the dynamic image tailcut cleaning.

## 2.2 Influence of the NSB level on the Image Parameters of the raw Crab 2001 Dataset

Figure 3 shows in the left graphs the average *WIDTH* (top) and *LENGTH* (bottom) as a function of the zenith angle (ZA) for raw Crab data taken with HEGRA CT1 in 2001.

On the right hand side the average *WIDTH* and *LENGTH* are drawn as a function of the pedestal RMS of the respective runs for zenith angles smaller than  $10^\circ$  (open circles) and for zenith angles larger than  $30^\circ$  (stars).

A similar effect is present in the observed hadronic data: at a given ZA the average *WIDTH* and *LENGTH* scale inversely to the pedestal RMS values, i.e. to the NSB level.

In the left hand side graphs of Figure 3 straight line fits have been added, their meaning and use is described in Section 3.

## 2.3 The comparison with Mkn 421

In Figure 4 we compare the Mkn 421 data of 2001 with the Crab data up to a ZA of  $15^\circ$ . Again the hadronic background's average values are calculated according to the prescriptions above.

The left plots show that the average *WIDTH* and *LENGTH* values of hadrons in the Mkn 421 dataset are considerably higher than those of the Crab dataset. This can be attributed to the lower NSB level around Mkn 421 compared to the Crab sky region.

The difference disappears when the average *WIDTH* and *LENGTH* are plotted versus the average pedestal RMS of

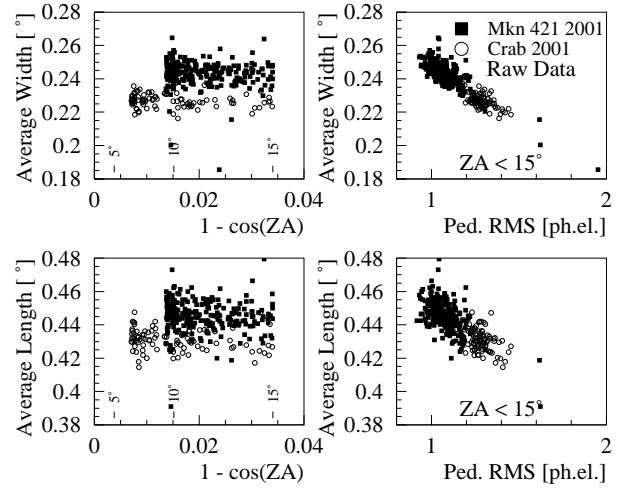


**Fig. 4.** Like Figure 3, except that Mkn 421 observations from 2000-2001 have been added and the ZA has been limited to  $15^\circ$ . The smaller average *WIDTH* and *LENGTH* values of the Mkn 421 data correspond to the lower NSB level around this source.

the runs: both distributions describe the same general dependency of the averaged *WIDTH* and *LENGTH* on the NSB level.

Two conclusions can be drawn from this plot:

1. Cuts that are optimised to extract a  $\gamma$ -signal from the Crab shall be inefficient on an uncorrected Mkn 421 dataset, as their average  $\gamma$ - *WIDTH* and *LENGTH* are too large.
2. The cuts shall extract different fractions of background in uncorrected datasets, when the NSB is varying. Thus the hourly background level under the signal peak shall be different e.g. for Mkn 421 and Crab in the uncorrected case and cannot efficiently be used to monitor this variable source.

## 3 An Attempt for the Correction

A clear correlation between the pedestal RMS and the distribution of the parameters *WIDTH* and *LENGTH* is visible for the Monte Carlo data and for the real data (besides the ZA dependence).

Therefore we tried the following correction Ansatz: the individual values of *WIDTH* and *LENGTH* were scaled with a factor that shifts the mean *WIDTH* and *LENGTH* values onto the reference ones drawn as lines in Figure 3.

In the following this is named as a **Zerth Order Nightsky noise Korrektion** (*zonk*).

To test the new method, a set of cuts was optimised on 'zonked' Crab data. The cut has been tried on uncorrected Crab data and both on 'zonked' and uncorrected Mkn 421 data. Table 1 summarises the results for ZAs up to  $25^\circ$ , Figures 5 and 6 show the corresponding alpha-plots.

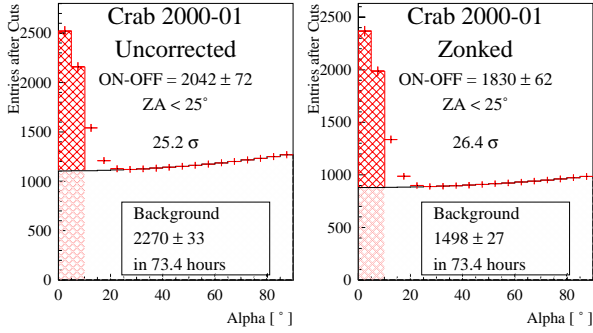


**Fig. 5.** Alphaplots of the Crab observation Oct. 2000 through Mar. 2001, uncorrected on the left hand side and 'zonked' on the right hand side.

As a result we obtain a more equalized background rate and a small improvement in significance for the 'zonked' data.

The gain in significance is smaller than we expected. We attribute this modest gain to:

- (i) the best correction has not yet been found
- (ii) for large statistics of runs this correction is partially averaged out.

The important result of Table 1 is that the background rates fluctuate much less.

It can be seen that the too low background rate in uncorrected Mkn 421 data, which stems from the too high values of *WIDTH* and *LENGTH*, is shifted towards the reference value of 'zonked' Crab data. In the uncorrected Crab data the hadronic background rate is found too high.

## 4 Discussion

In summary, the following improvements have been achieved with the first simple Ansatz of correction:

- (i) An improvement in the  $\gamma$ -hadron separation cuts.
- (ii) After the correction very similar hadronic background rates have been found under different NSB conditions.
- (iii) As a byproduct we note that the procedure for the cut optimisation was much more stable and converging faster.

Data	Sign.	$\gamma s$	$\gamma$ -rate	Bg	Bg-rate
Crab <i>zonk</i>	$28.6\sigma$	1830	24.7/h	1498	<b>20.4/h</b>
Crab 'as is'	$26.9\sigma$	2042	27.8/h	2270	30.0/h
M-421 <i>zonk</i>	$63.6\sigma$	7572	45.2/h	3302	<b>19.7/h</b>
M-421 'as is'	$61.8\sigma$	6290	37.5/h	2028	12.1/h

**Table 1.** Summary of improvements for the 'zonk' method: significance (Sign.), excess  $\gamma s$ , background (Bg) and rates. Results are given for Crab and Mkn 421, for the 'zonked' and uncorrected data. In all cases the same cut was applied.

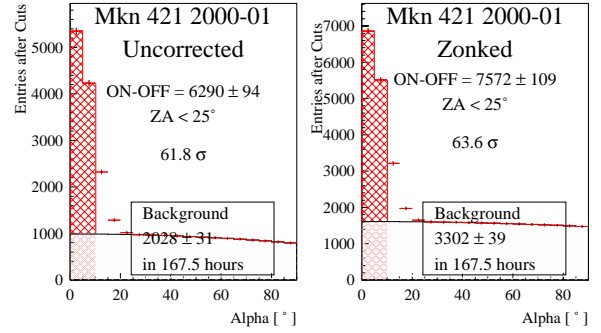


**Fig. 6.** Alphaplots of the Mkn 421 observation Jan. through May. 2001, uncorrected on the left hand side and 'zonked' on the right hand side.

- (iv) It should be noted that this correction is not identical to the ON-OFF procedure used by many collaborations because the ON-OFF procedure does not take changes in the NSB directly into account.

At very large ZAs ( $\gtrsim 50^\circ$ ) we observe in La Palma in general a dramatic increase in NSB. This effect might need a more detailed study before being included into the correction.

We plan for the next steps to refine the approach by taking into account the threshold effects and corrections for stronger variations of the NSB such as from the moonlight.

*Acknowledgements.* We would like to thank Dorota Sobczyńska for the provision of the Monte Carlo simulation.

## References

- Mirzoyan, R. et al., 1994, NIMA **351**, 513
- Cortina, J. et al., 1999, in Proc. GeV-TeV Gamma Ray Astrophysics Workshop (Snowbird), ed. Dingus B. L., et al., 368
- Hillas, A. M., 1985, in Proc. 19th ICRC (La Jolla), **3**, 445
- Petry, D., 1997, PhD Thesis, MPI-preprint MPI-PHE/97-27, Technische Universität München
- Kranich, D., 2001a, PhD Thesis, Technische Universität München
- Kranich, D., et al., 2001b, these proceedings